PCCP

Application of the two-step model to the diffusion of linear diatomic and triatomic molecules in silicalite

Pierfranco Demontis,*[a] Jörg Kärger,[b] Giuseppe B. Suffritti[a] and Antonio Tilocca[a]

[a] *Dipartimento di Chimica, Università degli Studi di Sassari, Via Vienna 2, I-07100 Sassari, Italy*
[b] *Fakultät für Physik und Geowissenschaften der Universität Leipzig, Linnéstraße 5, D-04103 Leipzig, Germany*

Received 14th September 1999, Accepted 4th January 2000
Published on the Web 8th March 2000

Molecular dynamics simulations of the diffusion of diatomic oscillators representing the halogen molecules and of linear flexible triatomic species modelling CO_2 and CS_2 have been carried out in the zeolite silicalite. The main purpose was to compare the performance of the random walk model to that of its "two-step" extension in representing molecular migration inside such an interconnected 3-D pore network. The two-step model always gives a better estimate of the elements of the diffusion tensor, and also provides some interesting insight into the features of the molecular motion of the studied species. The analysis of the two-step event probabilities is also applied to assess the extent of diffusive memory in each case.

1. Introduction

The special pore structure of the zeolite silicalite has deep effects on the diffusive properties of guest molecules moving in its cavities. The main consequence is that the one-dimensional components D_x, D_y and D_z of the total diffusion coefficient must depend on each other. By representing the motion of sorbed molecules as a random walk between neighbouring channel intersections, a simple correlation rule has been obtained.[1] This representation does not imply any assumption about where the molecules spend most of their time. One is simply approaching the real trajectory by a sequence of straight lines connecting the channel intersections. For displacements much larger than the distances between adjacent intersections, this approximation does in no way affect the resulting diffusivities. The basic assumption of the random walk model is the quick loss of memory of the diffusants between consecutive "jumps" (*i.e.* on the way from one intersection to the subsequent one); this corresponds to a complete randomisation of molecular migration, in such a way that, after entering a channel intersection, a molecule will proceed to any of the four adjacent intersections with a probability independent of its previous "history".

If this assumption is not entirely fulfilled, one can expect deviations from the behaviour predicted on the basis of the random walk propagation. As these deviations are, at least partially, due to the persistence of diffusive memory in the sorbates, they can be taken into account by representing the diffusive path as a sequence of *two*-step (instead of *single*-step) events: each event is a pair of jumps between adjacent intersections (see ref. 2). By considering only such coupled displacements in the overall trajectory, as a first approximation, the correlation between *two* subsequent displacements from channel intersection to channel intersection can be directly accounted for. Indeed, by expressing the components of the mean square displacement on the basis of the observed numbers of different two-step events, we implicitly avoid the assumption of complete randomisation between single jumps. For example, the tendency of a molecule to continue (or not to continue) in the same direction from which it came is directly considered in the two-step model equations, which include the numbers of coupled events in the same direction, as well as the switches of direction, and so on. In other words, the diffusive memory can (if present) affect the diffusion coefficients estimated through the two-step model, while in the random walk model such influence cannot be directly included.

Both models are statistical tools to analyse and interpret the data produced by molecular dynamics (MD) simulations; while in the random walk model the jump probabilities are fixed *a priori*, the new model is built over two-step probabilities derived from the MD trajectory, thus establishing a direct link between "experiment" (*i.e.*, the MD trajectory) and theory (the model). The simulations provide the input data needed to apply the statistical models, which can then be used to study in detail the diffusive behaviour and dynamical phenomena such as correlation effects. The investigation of the existence and extent of correlation effects is an important problem, for instance to test the applicability of stochastic jump diffusion models (JDM)[3–5] to study diffusive phenomena in zeolites over much longer time scales than those currently accessible by standard MD simulations. JDM models are based on the assumption of uncorrelated jumps between sites; however it is possible to include correlation effects in such models by modifying them on the basis of correlation factors determined analytically[5] or by MD simulations.[6] The study of the deviations from the behaviour predicted by random walk correlation rules may also highlight some particular aspects of the diffusive process. The observation that the diffusion anisotropy experimentally determined in chabazite is larger than expected on the basis of uncorrelated propagation may suggest the existence of additional transport barriers hindering diffusion along z.[7]

In a previous work[2] we applied the two-step model to the diffusion of ethane in silicalite; the effect of varying the sorbate loading and the system temperature was studied through MD simulations. In this paper, the same analysis is carried out to study the diffusive behaviour of diatomic and triatomic linear species in silicalite at infinite dilution. Therefore, here we test the effect of changing the sorbate mass and size, while keeping constant the temperature (300 K) and the loading (one molecule sorbed in two silicalite unit cells). The

performances of the random walk and two-step models are tested by comparing the corresponding mean square displacements (MSD) and diffusion coefficients with those obtained through the standard analysis of MD trajectories (see below). The possible effect of a more complex internal structure, as in the case of linear triatomic species, is also considered. The diatomic species studied model the three halogen molecules, chlorine, bromine and iodine, while the triatomic molecules represent carbon dioxide and carbon disulfide. Both the zeolite framework and the sorbed molecules are considered as fully flexible.

2. Details of the calculations

Silicalite is the all-silica analogue of the synthetic zeolite catalyst ZSM-5. Two different channel systems made of 10 oxygen rings (with connecting Si atoms) with diameter of about 5.5 Å are the main feature of its framework topology. Straight channels run parallel to [010] direction, while sinusoidal channels have an average direction along [100]. The channel intersections, which allow the 3-D motion of sorbed molecules, are elongated cavities of about 9 Å diameter. We represented the silicalite crystal structure, according to X-ray diffraction studies,[8] in the *Pnma* space group (orthorhombic), with unit-cell lattice parameters $\boldsymbol{a} = 20.022$ Å, $\boldsymbol{b} = 19.899$ Å, $\boldsymbol{c} = 13.383$ Å. Fig. 1 schematically shows the structure of silicalite; the continuous lines represent the axes of the zigzag channels (in *x*-direction) and of the straight channels (in *y*-direction)

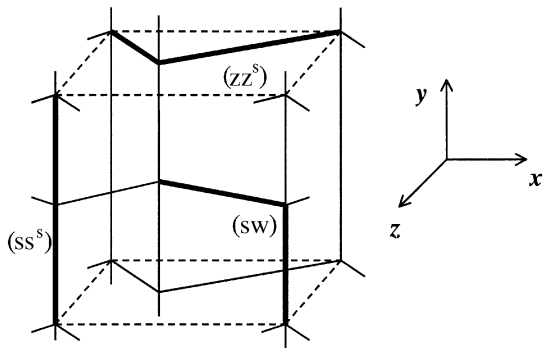

Fig. 1 Schematic representation of the channels geometry in a silicalite unit cell; channels are represented by continuous lines. The three main coupled displacements are shown as thick lines: (ss^s), two displacements in straight channels, in the same *y* direction; (sw), a switch from a straight to a zigzag channel, or *vice versa*; (zz^s), two displacements in zigzag channels, in the same *x* direction.

respectively. The simulation box consisted of two silicalite unit cells superimposed along *z*, resulting in 576 framework atoms (192 Si and 384 O). The full flexibility of the silicalite lattice was accounted for by a harmonic model, described in detail in refs. 9 and 10.

A Morse potential always describes the intramolecular bond of the diatomic species, with parameters derived from spectroscopic data,[11] while the harmonic intramolecular potential of Zhu and co-workers has been adopted to model CO_2 and CS_2.[12,13] We verified that this simple potential gives an excellent reproduction of the vibrational spectra of both triatomic molecules. The intramolecular potential functions and parameters are reported in Table 1.

The Lennard-Jones (LJ) potential is used to model all the intermolecular interactions between the atoms of the sorbates and the silicalite oxygens (no interactions between the sorbed species are present; the interactions with the silicon atoms are neglected, because they are well shielded by the oxygen atoms covering the surface of the channels). For the diatomic species, the Cl–O, Br–O and I–O parameters are the same as for Ar–O, Kr–O and Xe–O.[14,15]

The self-interaction LJ parameters of Murthy *et al.*[16] for carbon and oxygen atoms in CO_2 describe their interaction with the oxygen atoms through the standard combining rules,[17] using the zeolite oxygens self-interaction parameters[18] ($\sigma = 2.529$ Å, $\varepsilon = 1.51$ kJ mol^{-1}). The Murthy intermolecular potential also includes a contribution due to the high quadrupole moment of CO_2. In our case only one CO_2 molecule is adsorbed and no intermolecular quadrupole–quadrupole interactions are present. Moreover, in our harmonic model the charges present on the framework atoms are not explicitly considered, and thus there is no contribution to the intermolecular energy arising from the effect of the intrazeolite electric field on the molecular quadrupole moment. The inclusion of this interaction would be essential if any Al atoms and charged counterbalancing cations were present, or if a very accurate representation of the CO_2 motion was sought, faithfully describing, for example, the way in which the additional attractive contribution may affect the effective pore size. In this work such an accurate description is not required, as we are interested in the effects of molecular shape, size and mass over the diffusive behaviour, and the models we use are mainly intended to represent diatomic and triatomic species of different size and mass. Therefore for CO_2 we approximated the quadrupole–framework interaction by scaling the well depths ε_{O-Ozeo} and ε_{C-Ozeo} by 1.5, so as to obtain a good reproduction of the experimental heat of adsorption[19] of CO_2 in silicalite, which is about 28 kJ mol^{-1}. This approximation leads to diffusion coefficients consistent with experimental

Table 1 Intramolecular potential functions and parameters

(a) Morse potential[a] parameters (diatomic molecules)

	r_{eq}/Å	β/Å^{-1}	D_e/kJ mol^{-1}
Cl_2	1.988	2.037	242.19
Br_2	2.28	1.964	192.044
I_2	2.666	1.867	148.703

(b) Harmonic potential[b] parameters (X–C–X triatomic molecules)

	r^c_{eq} /Å	θ^d_{eq} /degrees	k_1/kJ mol^{-1} Å^{-2}	k_2/kJ mol^{-1} Å^{-2}	k_θ/kJ mol^{-1}
CO_2	1.161	180	4664.7	782.4	231.3
CS_2	1.56	180	2258.2	361.3	171.5

[a] $V(r) = D_e\{[1 - \exp(-\beta(r - r_{eq}))]^2 - 1\}$. [b] $V = k_1[(r_{C-X1} - r_{eq})^2 + (r_{C-X2} - r_{eq})^2] + k_2(r_{C-X1} - r_{eq})(r_{C-X2} - r_{eq}) + k_\theta(\theta - \theta_{eq})^2$. [c] Equilibrium C–X bond length. [d] Equilibrium X–C–X angle.

Table 2 Intermolecular (guest–host) Lennard-Jones potential[a] parameters

Interaction	σ/Å	ε/(kJ mol^{-1}
Cl–O	3.029	1.028
Br–O	3.14	1.335
I–O	3.2745	1.737
C(CO_2)–O	2.657	0.739
O(CO_2)–O	2.772	1.251
C(CS_2)–O	2.940	0.8015
S(CS_2)–O	3.025	1.516

[a] $V(r) = 4\varepsilon[(\sigma/r)^{12} - (\sigma/r)^6]$.

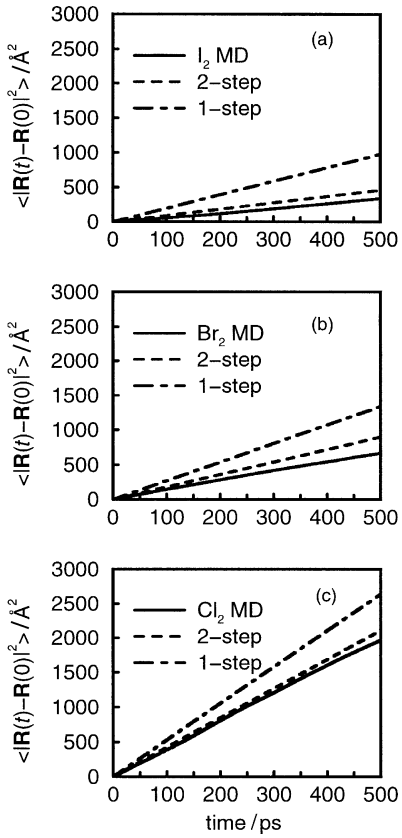

Fig. 2 Mean square displacement curves obtained according to two-step model (dashed line), one-step model (dot-dashed line) and eqn. (1) (solid line), for the halogen molecules: (a) I_2, (b) Br_2, (c) Cl_2.

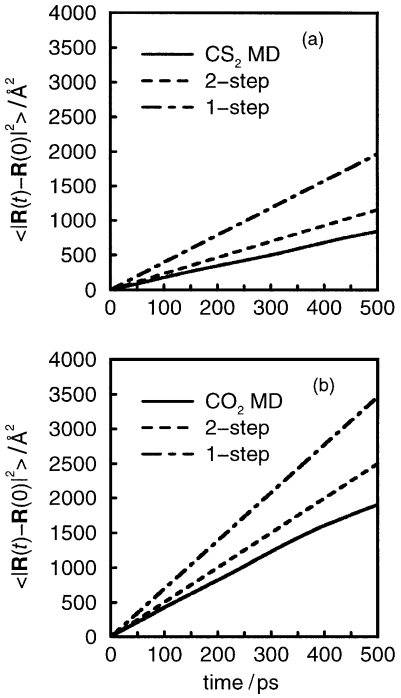

Fig. 3 The same as Fig. 2, for the triatomic molecules: (a) CS_2, (b) CO_2.

data (see below). However it is likely that at finite loadings, with important quadrupole–quadrupole interactions, this kind of approximation may lose its validity. Our model should be considered as representing a linear triatomic molecule, comparable to carbon dioxide only at infinite dilution, in a neutral environment.

On the other hand, the Tildesley–Madden[20] LJ parameters for carbon and sulfur in CS_2 have been taken without modifications, as in their paper CS_2 is modelled through a non-quadrupolar, effective three-site potential. All the intermolecular LJ parameters are reported in Table 2.

In each case the system was equilibrated in the micro-canonical ensemble at $T = 300$ K for 900 ps, then a production run of 20 ns was carried out using a time step of 1 fs. The guest coordinates and velocities were stored every 32 fs.

The diffusion coefficients were calculated in the standard way[17] by fitting the MSD curves, calculated by eqn. (1), to a

Table 3 Diffusion coefficients (10^{-8} m^2 s^{-1}) calculated through: (a) the standard MD method; (b) the random walk model and (c) the two-step model

		D	D_x	D_y	D_z
Cl_2	(a)	0.67 ± 0.09	0.73 ± 0.14	1.1 ± 0.3	0.14 ± 0.04
	(b)	0.87	1.15	1.2	0.27
	(c)	0.70	0.81	1.1	0.19
Br_2	(a)	0.22 ± 0.04	0.22 ± 0.06	0.37 ± 0.09	0.062 ± 0.02
	(b)	0.44	0.70	0.49	0.13
	(c)	0.30	0.39	0.42	0.083
I_2	(a)	0.11 ± 0.01	0.095 ± 0.02	0.22 ± 0.04	0.027 ± 0.006
	(b)	0.327	0.337	0.55	0.0955
	(c)	0.155	0.16	0.261	0.0452
CO_2	(a)	0.66 ± 0.11	0.58 ± 0.12	1.25 ± 0.3	0.16 ± 0.03
	(b)	1.17	1.64	1.5	0.36
	(c)	0.85	0.99	1.3	0.24
CS_2	(a)	0.28 ± 0.05	0.19 ± 0.04	0.59 ± 0.15	0.06 ± 0.01
	(b)	0.656	0.84	0.92	0.20
	(c)	0.386	0.44	0.62	0.10

straight line in the 50–500 ps region and then applying the Einstein equation (2):

$$\Delta r^2(t) = \frac{1}{N}\sum_{i=1}^{N} |\boldsymbol{r}(t_i + t) - \boldsymbol{r}(t_i)|^2 \quad (1)$$

$$D = \lim_{t\to\infty} \frac{\Delta r^2(t)}{2dt} \quad (2)$$

N in eqn. (1) is the total number of time origins spaced by t; in eqn. (2), d is the corresponding dimensionality, *i.e.*, 3 for the total diffusion coefficient, and 1 for its components.

The MSD estimated by the one- and two-step models are given by eqns. (3)–(5) and (6)–(8), respectively, as a function of the observed numbers of single and double displacements between neighbouring intersections:[2]

$$\langle \Delta x^2(t)\rangle = n_z(t)(a/2)^2 \quad (3)$$

$$\langle \Delta y^2(t)\rangle = n_s(t)(b/2)^2 \quad (4)$$

$$\langle \Delta z^2(t)\rangle = n_s(t)n_z(t)/n(t)(c/2)^2 \quad (5)$$

and

$$\langle \Delta x^2(t)\rangle = n^s_{zz}(t)a^2 + n_{sw}(t)(a/2)^2 \quad (6)$$

$$\langle \Delta y^2(t)\rangle = n^s_{ss}(t)b^2 + n_{sw}(t)(b/2)^2 \quad (7)$$

$$\langle \Delta z^2(t)\rangle = n_{sw}(t)(c/2)^2 \quad (8)$$

Here: $n(t)$ is the total average number of single steps observed in an interval t; $n_z(t)$ is the average number of single steps in the zigzag channel; $n_s(t)$ is the average number of single steps in the straight channel; $n^s_{zz}(t)$ is the average number of double steps in the zigzag channel (and in the same direction); $n^s_{ss}(t)$ is the average number of double steps in the straight channel (and in the same direction); and $n_{sw}(t)$ is the average number of straight-to-zigzag, or *vice versa*, double steps, *i.e.*, $n_{sw}(t) = n_{sz}(t) + n_{zs}(t)$. Examples of such coupled displacements are shown as thick lines in Fig. 1.

The MSD curves are shown in Fig. 2 for the halogens and in Fig. 3 for CO_2 and CS_2, while the calculated diffusion coefficients are reported in Table 3. The errors reported in Table 3 for the diffusion coefficients obtained by the standard method have been calculated from a block analysis of data,[21] by dividing the trajectory in 20 blocks of 1 ns each and computing the percent error according to the formula:

$$\delta D\% = \left(\frac{1}{m(m-1)}\sum_{i=1}^{m}(D_i - \bar{D})^2\right)^{1/2}\frac{100}{\bar{D}}, \quad (9)$$

where m is the number of blocks, and D_i is the diffusion coefficient relative to the ith block. The computed errors vary between 13 and 28%, being usually lower for the total D values.

The number of events as a function of the time has been calculated as described in ref. 2. After mapping the sequence of N_i intersections visited by the molecule, the trajectory was then analysed in the following way:

(1) The index j run from 2 to N_i.

(2) All the sequences of j intersections included in the full (N_i) one were separately studied, so as to obtain the average number and duration of each kind of event observed in a typical sequence of j intersections.

(3) The time τ needed to cross j intersections was simultaneously averaged over all such sequences, and the average numbers of events found in the path along N_i intersections were then assigned to the time τ.

In this way it was possible to account for the time dependence of the event numbers, required in order to apply eqns. (3)–(5) and (6)–(8). Table 4 reports the number of events and their relative probabilities, while in Table 5 the mean time lengths of each event are shown.

The numbers reported in the tables correspond to $\tau \sim 1$ ns; while in such a time interval the number of two-step events observed may be rather low, in particular for iodine, we verified that the calculated MSD and the main conclusions drawn below do not change appreciably when taking, for example,

Table 4 Event numbers and probabilities (after $\tau \sim 1$ ns); probabilities are shown as *bold italic* numbers

	n_s	n_z	n^s_{ss}	n^o_{ss}	n^s_{zz}	n^o_{zz}	n_{sw}	n_{sz}	n_{zs}	n_1	n_2
Cl_2	26.223 ***0.52***	23.777 ***0.48***	3.790 ***0.15***	4.888 ***0.20***	1.968 ***0.08***	5.487 ***0.22***	8.866 ***0.35***	4.433 ***0.175***	4.434 ***0.175***	50.0	25.0
Br_2	10.761 ***0.43***	14.239 ***0.57***	1.335 ***0.11***	2.148 ***0.17***	1.030 ***0.88***	4.192 ***0.34***	3.795 ***0.30***	1.897 ***0.15***	1.898 ***0.15***	25.0	12.5
I_2	11.977 ***0.63***	7.023 ***0.37***	0.908 ***0.097***	4.042 ***0.42***	0.303 ***0.033***	2.169 ***0.23***	2.078 ***0.22***	1.041 ***0.11***	1.037 ***0.11***	19.0	9.5
CO_2	32.154 ***0.49***	32.846 ***0.51***	4.215 ***0.13***	6.37 ***0.196***	2.193 ***0.067***	8.738 ***0.269***	10.985 ***0.338***	5.494 ***0.169***	5.491 ***0.169***	65.0	32.5
CS_2	19.896 ***0.54***	17.104 ***0.46***	2.218 ***0.12***	5.466 ***0.295***	1.16 ***0.063***	5.128 ***0.28***	4.528 ***0.245***	2.263 ***0.122***	2.266 ***0.122***	37.0	18.5

Table 5 Event time lengths (picoseconds)

	t_s	t_z	t^s_{ss}	t^o_{ss}	t^s_{zz}	t^o_{zz}	t_{sw}	t_{sz}	t_{zs}	t_1	t_2
Cl_2	19.3	21.9	37.7	38.8	46.4	41.2	42.6	41.2	44.0	20.6	41.1
Br_2	36.7	42.9	72.9	64.8	111.5	76.6	88.2	80.6	95.7	40.3	80.6
I_2	47.5	66.0	101.4	88.9	122.2	133.8	122.4	104.6	140.4	54.4	108.9
CO_2	14.6	16.4	28.5	26.5	38.8	29.3	34.4	32.9	35.9	15.5	31.0
CS_2	26.4	28.8	60.0	46.9	78.0	50.7	61.5	57.4	65.6	27.5	55.0

$\tau \sim 5$ ns. Indeed, as in a typical correlation function calculation, the number of sequences accounted for decreases with increasing time, becoming one for $\tau = \tau_{RUN}$ (*i.e.*, $j = N_i$), and the statistical accuracy gets worse. Therefore, the advantage of working on a greater number of events is counterbalanced by a worse statistics. The superscript "s" is used in Table 4 and Table 5 to identify consecutive events in the "same" direction, while "o" stands for "opposite" direction. Notwithstanding the fact that the latter events do not take part in the overall motion of the molecule [indeed, they are not included in eqns. (6)–(8)], they are important for a qualitative discussion of the diffusive motion. The last two columns report the total number (time length) of single- and two-step events, respectively. The overall time length of single jumps was calculated as:

$$t_1 = p_s t_s + p_z t_z \tag{10}$$

while for the coupled events we have:

$$t_2 = p^s_{ss} t^s_{ss} + p^o_{ss} t^o_{ss} + p^s_{zz} t^s_{zz} + p^o_{zz} t^o_{zz} + p_{sw} t_{sw} \tag{11}$$

where the symbols are as in eqns. (3)–(8); p^s_{ss} and t^s_{ss} are the probability and mean time length of double steps in the straight channel (and in the same direction); and so on.

3. Discussion of results

Qualitative analysis of the molecular motion

Table 4 and Fig. 4 show that in general coupled displacements in the opposite direction ("bouncing-backs") are more likely than those in the same direction; the switches (s–z or z–s) are roughly half-way between these two events. Two different trends are observed:

$$p^o_{zz} > p^o_{ss} > p_{sz} > p^s_{ss} > p^s_{zz} \quad \text{for } Cl_2, Br_2 \text{ and } CO_2 \tag{12a}$$

$$p^o_{ss} > p^o_{zz} > p_{sz} \sim p^s_{ss} > p^s_{zz} \quad \text{for } I_2 \text{ and } CS_2 \tag{12b}$$

The longer molecules (iodine and carbon disulphide) have a lower tendency to switch direction; this could be connected to the greater diffusive memory for such species. In order to highlight possible memory effects, we could ignore the displacements in opposite directions and directly compare the p^s_{ss} and p_{sz} numbers, as well as p^s_{zz} and p_{zs} ones. If the propagation is completely uncorrelated, the following expressions[2] must hold:

$$p_{sz} = p_s p_z = p_{zs} \qquad p^s_{ss} = \tfrac{1}{2} p_s^2 \qquad p^s_{zz} = \tfrac{1}{2} p_z^2 \tag{13}$$

hence:

$$\frac{p^s_{ss}/p_{sz}}{p_s/2p_z} = \frac{p^s_{zz}/p_{zs}}{p_z/2p_s} = 1 \tag{14}$$

Any deviation from unity of the "randomisation" ratios in eqn. (14) is to be ascribed to correlations in the diffusive motion; a ratio >1 denotes a tendency to keep the direction of motion, while a ratio <1 denotes a preference to "turn the corner". With the separate analysis of the two ratios we can independently investigate the diffusion in the two channel systems, so as to avoid confusions due to the different numbers of straight or zigzag sections visited. At the same time, not including the bouncing-backs in the comparison, we are somewhat isolating the other two kinds of events, allowing a better comparison, which would otherwise be obscured by the overwhelming number of displacements in opposite directions. [We are implicitly assuming that the only role of the "bouncing-backs" is to uniformly reduce the total numbers of continuations and switches, which actually are the only relevant events (eqns. (6)–(8)).]

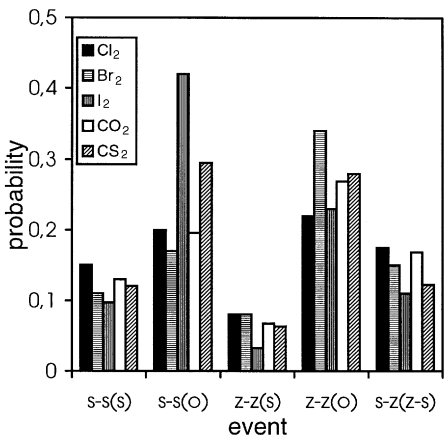

Fig. 4 Histograms of the two-step event probabilities for diatomic and triatomic molecules.

Table 6 shows that in the straight channel the "continuations" are usually more probable than the switches, while in the zigzag channel there is a better randomisation of the motion. Obviously, the channels shape is involved in this phenomenon. The motion of the heaviest molecule, iodine, is practically uncorrelated in *both* channel systems, probably due to the longer residence times that allow a better thermalisation. On the other hand the longest molecule considered, CS_2, shows considerable diffusive memory in both channels, tending to maintain the direction of motion: the longer molecular axis acts as an effective guide to direct the molecular propagation. When moving in the zigzag channel no molecule except CS_2 shows any preferential tendency to continue its motion along the channel, and bromine and CO_2 actually prefer to "turn the corner". Clearly, correlated jumps must arise from an insufficient thermalisation between jumps, but this lack of thermalisation may in turn be strongly affected by some further parameters, such as the molecular shape and dimensions, as well as the intermolecular interactions.

From this perspective it is remarkable that the trend in eqn. (12a) is the same as previously found for ethane at different loadings;[2] furthermore, the diffusion coefficients obtained[2] for ethane at 1 molecule per unit cell and for chlorine and carbon dioxide at infinite dilution (Table 3) are quite comparable, in spite of the different masses and sizes. Several factors, with opposite effect, could be involved in this point, such as the higher loading for ethane, and the differences in the single LJ parameters for the interaction with the zeolitic host. The calculated heats of adsorption are reported in Table 7, while for ethane we found, at 1 molecule per unit cell, $q = 30$ kJ mol^{-1}. The observed trend, $q(Cl_2) < q(CO_2) < q(C_2H_6)$, may partially counterbalance the (inverse) order of the masses, leading to

Table 6 Randomisation ratios in the two channel systems

	$(p^s_{ss}/p_{sz})/(p_s/2p_z)$	$(p^s_{zz}/p_{zs})/(p_z/2p_s)$
Cl_2	1.59	1.00
Br_2	1.92	0.80
I_2	1.03	1.03
CO_2	1.60	0.77
CS_2	1.66	1.24

Table 7 Calculated heats of adsorption[a]

	q/kJ mol^{-1}
Cl_2	25.1
Br_2	37.6
I_2	58.4
CO_2	27.3
CS_2	45.2

[a] $q = -(\langle U_{g-h} \rangle - RT)$.

very similar diffusion coefficients. However, a simpler line of reasoning could take into account only the molecular length, defined as $r_{eq} + \sigma_{X-Ozeo}$ (X being Cl, Br or I) for the diatomic molecules and as $2r_{eq} + \sigma_{X-Ozeo}$ (X being O or S) for the triatomic species. One obtains $\sim$5 Å for ethane and Cl_2, 5.1 Å for CO_2, 5.4 Å for Br_2, 5.9 Å for I_2, and 6.1 Å for CS_2. On the basis of the molecular length alone, Cl_2, CO_2 and ethane may be put roughly on the same level. The above observations seem to indicate that the effective length of the molecule can play an important role in determining the diffusive properties of linear molecules in silicalite.

The average event time lengths, reported in Table 5 and as histograms in Fig. 5, give further insight into the diffusion mechanism. Clearly, the absolute values of these propagation times are mainly determined by the masses, but the relative speed of the different events for each species can in any case be of some interest. The fastest events are always the bouncing-backs along the straight channels, while the slowest are the consecutive displacements in the same direction along the zigzag channel, except for iodine, whose slowest two-step event is the bouncing-back along the zigzag channel. CS_2 (whose trend of event probabilities was similar to I_2) shows a trend closer to the smaller species than to iodine, reflecting the greater importance of the molecular weight in determining the event time lengths. It is worth noting that $t_{zs} > t_{sz}$ in all cases, with larger differences for the longer species, while as shown in Table 4, $p_{zs} \sim p_{sz}$, as to be expected on the basis of the time reversibility.

This point deserves some comments. The time length of a two-step event is calculated as the difference between the time of access to the last intersection (C in Fig. 6) minus the time of access to the starting (A) intersection. Therefore the "forward" z–s event, starting at t_0 and ending at t_2, is distinct from the corresponding "backward" s–z sequence of jumps, which starts at t_3 and is completed at t_1. Time reversibility strictly applies only to the fragment of trajectory between t_1 and t_2, and we have indeed verified that the time length of s–z and z–s events would be the same if calculated in such a region, *i.e.* between the access to the last intersection and the *exit* from the first one.

These phenomena can be further investigated by looking at the decay of the autocorrelation function of the end-to-end versor $\hat{\boldsymbol{u}}(t)$[22,23] directed along the molecular axis:

$$C(t) = \langle \hat{\boldsymbol{u}}(t) \cdot \hat{\boldsymbol{u}}(0) \rangle \quad (15)$$

In silicalite, decorrelation of the u_x and u_y components can only come about through interconversions from one channel type to another, while the u_z component is usually decorrelated in a shorter time, due to the rattling motion of the molecules in the channels, corresponding to fast oscillations of u_z around zero. We calculated the decorrelation times by fitting a straight line to the logarithm of the normalised autocorrelation function of the components of $\hat{\boldsymbol{u}}(t)$. Assuming an exponential relaxation, the slope of the straight line matches $-1/\tau_d$, τ_d being the decorrelation time.

Actually, this method gives good results only for the longer species, iodine and CS_2. The total correlation functions are shown in Figs. 7 and 8; the slow decay of the iodine and CS_2 functions is due to the slow decorrelation of their x and y

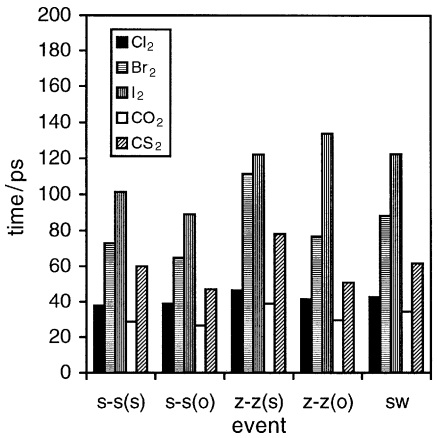

Fig. 5 Histograms of the two-step time lengths for diatomic and triatomic molecules.

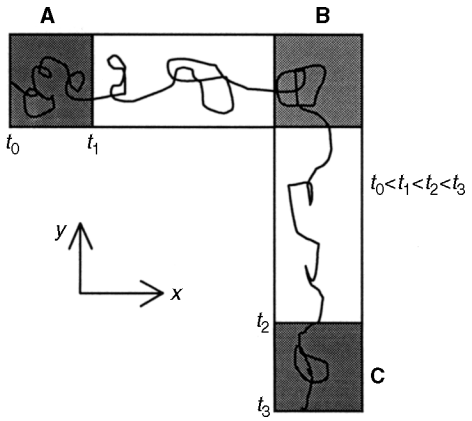

Fig. 6 Schematic representation of a switch of channel; the shaded regions represent the intersections crossed by the molecule.

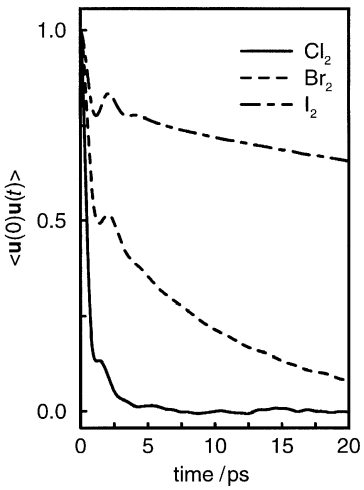

Fig. 7 Total autocorrelation functions of the end-to-end versor for the halogen molecules.

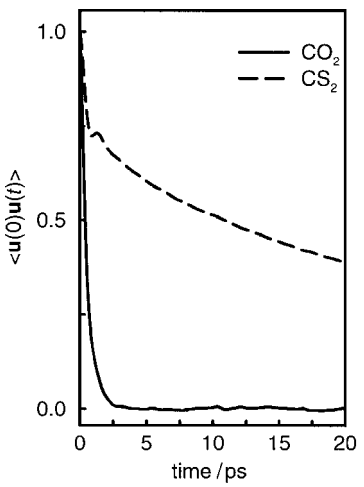

Fig. 8 The same as Fig. 7, for the triatomic molecules.

components. For the shorter species the decay is so fast, even along x and y, that it should be almost completely ascribed to the hindered rotations in the channels, rather than to actual straight–zigzag (or *vice versa*) migrations, and it could not provide reliable information about such processes. For the longer species the librations are less important and the orientational decorrelation is mostly determined by the switches of channel. Therefore, we report in Table 8 the values obtained for bromine, iodine and CS_2 only. For the longer species τ_x is considerably greater than τ_y, in agreement with the previous discussion and with the results of earlier MD simulations of n-butane and n-hexane in silicalite,[22,23] while for bromine τ_y is slightly larger than τ_x. Recall that t_{zs} and t_{sz} are solely determined by the migrations between different types of channels, while the decay of $C(t)$ can also be brought about by the librations in a single channel or intersection. Therefore it seems that only for the longest molecules, I_2 and CS_2, is the decorrelation of the end-to-end versor completely determined by the channel interconversions.

Comparison of the diffusion models

As shown in Figs. 2 and 3, the MSD curves reproduced by the two-step model are always considerably closer to the "standard" one than those obtained by the random walk model. As already found in the ethane case,[2] Table 3 shows that both jump models always overestimate the standard values of the diffusion coefficients; however, those predicted according to the two-step model are in much better agreement with the reference equations (1) and (2), which in turn should provide a good estimate of the "real" (experimental) values. For example, in recent uptake measurements to complete loading, Kocirík *et al.*[24] estimated the lower limit of the diffusion coefficient of iodine in silicalite as 10^{-12} m^2 s^{-1}, which is clearly not in contrast with our results. The diffusion coefficient for CO_2 in silicalite at 300 K and $\sim$12 molecules per unit cell has been determined through pulsed field gradient nuclear magnetic resonance (PFG-NMR)[25] and frequency response[26] methods; the measured values (0.2 and 0.3 $\times$ 10^{-8} m^2 s^{-1}, respectively) are of the same order of magnitude as ours ($0.66 \pm 0.11 \times 10^{-8}$ m^2 s^{-1}). The difference could be entirely ascribed to the considerable loading present in the experimental measure, since the NMR self-diffusivity of small molecules in silicalite usually shows a decreasing trend with increasing concentration,[27] due to the increasing mutual hindrance of the molecules. The diffusion anisotropy is not well accounted for by the random walk model, which gives D_y considerably larger than D_x only for I_2; actually, the two-step model also fails to reproduce well such effect in the bromine case, where it gives $D_y \sim D_x$ (but the random walk model in this case behaves even worse, predicting $D_x > D_y$).

The application of the random walk correlation rule, eqn. (16), and of the modified correlation rule,[2] eqn. (17),

$$a^2/D_x + b^2/D_y = c^2/D_z \tag{16}$$

$$\frac{a^2}{D_x}\left(1+\frac{4\Delta n^{s}_{zz}}{n_z}\right)+\frac{b^2}{D_y}\left(1+\frac{4\Delta n^{s}_{ss}}{n_s}\right)=\frac{c^2}{D_z}\left(1+\frac{2\Delta n_{sw}}{n}\right) \tag{17}$$

to the calculation of D_z from the D_y and D_x values obtained through the standard method [*i.e.*, those denoted as (a) in Table 3], gives rise to the values reported in Table 9. The Δn in eqn. (17) are the differences between the observed two-step event numbers and their values predicted according to a random walk (uncorrelated) propagation;[2] they are reported in Table 10. The Δ values are always non-zero, thus the random walk assumption of uncorrelated propagation is not fulfilled. Nevertheless, *both* correlation rules are always fairly adequate: the smaller Cl_2 and CO_2 species give higher errors; in the other cases the agreement is satisfactory. At the same time, we saw before that the direct calculation of total and one-dimensional diffusion coefficients through the two-step model gave much better results than the one-step model. This apparent discrepancy needs an explanation.

The random walk equations (3)–(5) considerably overestimate the one-dimensional MSDs. The MSD of a molecule after N jumps is:

$$\langle \Delta r^2(N)\rangle = \left\langle \left| \sum_{n=1}^{N} \boldsymbol{r}(n) \right|^2 \right\rangle = \sum_{n=1}^{N} \langle |\boldsymbol{r}(n)|^2\rangle + 2\sum_{n=1}^{N-1}\sum_{n=1}^{N-n} \langle \boldsymbol{r}(n)\cdot\boldsymbol{r}(n+n')\rangle, \tag{18}$$

and the random walk model neglects the cross terms in eqn. (18), assuming that the loss of memory is complete before each jump. However, Table 3 shows that:

$$\langle x^2(n_z)\rangle_{MD} < \left\langle \sum_{n=1}^{n_z} x(n)^2 \right\rangle = n_z\left(\frac{a}{2}\right)^2 \tag{19}$$

(the same is found for the other components), revealing that the contribution of cross terms in eqn. (18) is non-negligible

Table 8 Decorrelation times of the end-to-end versor and of its components

	τ/ps	τ_x/ps	τ_y/ps	τ_z/ps)
Br_2	11.5	9.3	13.1	3.5
I_2	123.1	183	101.5	11.8
CS_2	31	41.8	26.4	3.4

Table 9 D_z values (10^{-9} m^2 s^{-1}) obtained by the standard method, by the first correlation rule [eqn. (16)] and by the modified correlation rule [eqn. (17)]

	D_z [standard]	D_z [eqn. (16)]	D_z [eqn. (17)]
Cl_2	1.38	2.00	1.83
Br_2	0.62	0.62	0.60
I_2	0.27	0.30	0.29
CO_2	1.57	1.77	1.75
CS_2	0.59	0.64	0.57

Table 10 Deviations of the two-step event numbers from their theoretical (uncorrelated) values; relative deviations are in parentheses

	Δn^{s}_{zz}	Δn^{o}_{zz}	Δn^{s}_{ss}	Δn^{o}_{ss}	Δn_{sw}
Cl_2	−0.86	2.66	0.35	1.45	−3.6
	(−0.44)	(0.48)	(0.09)	(0.30)	(−0.41)
Br_2	−1.0	2.16	0.18	0.99	−2.33
	(−0.97)	(0.51)	(0.13)	(0.46)	(−0.61)
I_2	−0.34	1.52	−0.98	2.15	−2.35
	(−1.12)	(0.70)	(−1.08)	(0.53)	(−1.13)
CO_2	−1.956	4.59	0.24	2.39	−5.26
	(−0.89)	(0.52)	(0.05)	(0.37)	(−0.48)
CS_2	−0.817	3.151	−0.457	2.791	−4.67
	(−0.70)	(0.614)	(−0.205)	(0.51)	(−1.03)

and negative. In other words, if two consecutive jumps in either channels follow opposite directions, the net displacement is clearly zero. Therefore, such a pair of jumps should be excluded from the $n_s(n_z)$ total number, but a *single* step model cannot take into account *two* consecutive jumps. However, when eqns. (3)–(5) are combined to obtain the first correlation rule, eqn. (16), one takes the ratio of the one-dimensional MSDs, and this operation partially corrects the overestimation. As a consequence, the correlation rule between D_x, D_y and D_z may often be adequate, *even when the one-dimensional MSDs are not*.

The random walk equations can be in error, as shown in Table 3, as well as in Figs. 2 and 3, but they are still fairly valid when combined to give eqn. (16). The two-step model expressions perform much better in the prediction of one-dimensional MSDs, because they exclude all the pairs of consecutive events in opposite directions: indeed, they overestimate the "real" MSDs to a much lesser extent. Roughly speaking, the two-step model includes in the sum of eqn. (18) the cross products $\boldsymbol{r}(n)\cdot\boldsymbol{r}(n+1)$, which have the largest weight in the overall sum. Actually, it cannot account for some higher order events which also give no net contribution to the overall motion, as for example two subsequent *pairs* of displacements in opposite directions. Therefore the two-step model also slightly overestimates the "true" MSDs. Clearly, a higher order N-step model, with $N > 2$, would give an almost perfect match with the standard MSD. However, as long as the correlation rules are concerned, it is not surprising that the modified correlation rule, eqn. (17), does not always improve the first rule, eqn. (16). In both rules, overestimation errors are partially cancelled out; these errors are much higher in the random walk expressions.

4. Conclusions

The MD trajectory of a molecule adsorbed in the zeolite pores provides a complete description of the diffusive event, through the MSDs and diffusion coefficients. The statistical models we considered are simple and effective tools to extract from the full trajectory the basic features of the diffusive behaviour, giving a more general and schematic description, where the molecular trajectory is separated into a series of jumps between neighbouring intersections. The validity of each model, and possibly of the underlying assumptions, can be assessed through the corresponding MSD curves determined on the basis of the event numbers extracted from the MD trajectory. These numbers are the input data needed by the models; they are inserted into the equations pertaining to a model, trying to reproduce the original MSD curves: a tight fit indicates that the description of the model is adequate.

The application of the two-step model to the diffusion of flexible, linear diatomic and triatomic species in silicalite at infinite dilution highlighted some interesting points. The effective molecular length is the main factor determining the two-step jump sequence. Indeed, iodine and CS_2 show a different trend in the event probabilities, compared to the shorter species. Furthermore, molecules with different characteristics but similar lengths, such as Cl_2, CO_2 and ethane, give rise to comparable behaviour and diffusion coefficients. On the other hand, the observed event time lengths closely follow the order of the molecular masses. However, for the longer species, it is possible to associate the decorrelation times of the end-to-end versor along x and y with the channel interchange time lengths, while the considerable librations of the shorter species do not allow such comparison.

It is often assumed that correlation effects should be important only for relatively long molecules, which can extend over the full channel length ($\sim$10 Å), tending to maintain the alignment for long times. Nevertheless, we found that a random walk description may be inaccurate even for linear, 5–6 Å long, molecules, as it is already evident, for example, from the non-negligible deviations of Table 10. The one-dimensional MSDs (and the corresponding diffusion coefficients) calculated according to the two-step model are always in better agreement with the "real" values (obtained by the standard analysis of MD trajectories), compared to the predictions of the random walk model. We emphasised the importance of consecutive displacements in opposite directions in determining such improvements. The two-step model, by excluding such ineffective displacements, can better reproduce the actual path of the molecule through the n^s_{ss}, n^s_{zz} and n_{sw} event numbers, instead of the single-step numbers n_s and n_z, which unavoidably include pairs of consecutive steps in opposite directions.

In other words, the overestimation of the simulated MSDs is due to negative correlation effects. While the random walk equations (3)–(5) do not consider such correlations at all, the two-step equations (6)–(8) take into account any possible correlation between two consecutive jumps. The fact that the two-step model still gives a non-negligible overestimation of the MSDs may suggest that the diffusive memory does not vanish completely after two jumps, but even for the short molecules studied three or more jumps (spanning over 30 Å) might be needed before they completely lose the diffusive memory. It is interesting to note that negative correlation effects emerge only at high loadings in Na-Y zeolites, where each jump leaves behind a vacancy which is likely to be reached again at the successive jump.[5,28] The present paper shows that the very different structure of silicalite (entailing different diffusive mechanisms and time scales) makes such negative correlations non-negligible even at infinite dilution.

On the other hand, the uncorrelated correlation rule is scarcely affected by such imperfection of the random walk expressions: both rules turn out to be fairly adequate in most studied cases. For this reason, the validity of eqn. (16) does not necessarily imply that the molecular propagation in silicalite may be described as a series of uncorrelated jumps. The large applicability of such a rule between the components of the diffusion coefficient arises from compensating mechanisms that seemingly extend the range of validity of the random walk rule.

Acknowledgements

Grateful acknowledgement is made to MURST, University of Sassari and Consiglio Nazionale delle Ricerche for financial support.

References

1 J. Kärger, *J. Phys. Chem.*, 1991, **95**, 5558.
2 J. Kärger, P. Demontis, G. B. Suffritti and A. Tilocca, *J. Chem. Phys.*, 1999, **110**, 1163.
3 S. M. Auerbach, N. J. Henson, A. K. Cheetham and H. I. Metiu, *J. Phys. Chem.*, 1995, **99**, 10600.
4 F. Jousse, S. M. Auerbach and D. P. Vercauteren, *J. Phys. Chem. B*, 1998, **102**, 6507.
5 C. Saravanan, F. Jousse and S. M. Auerbach, *J. Chem. Phys.*, 1998, **108**, 2162.
6 F. Jousse, L. Leherte and D. P. Vercauteren, *J. Phys. Chem. B*, 1997, **101**, 4717.
7 N.-K. Bär, J. Kärger, H. Pfeifer, H. Schäfer and W. Schmitz, *Micropor. Mesopor. Mater.*, 1998, **22**, 289.
8 H. van Konigsveld, H. van Bekkum and J. C. Jansen, *Acta Crystallogr. B*, 1987, **43**, 127.
9 P. Demontis, G. B. Suffritti, S. Quartieri, E. S. Fois and A. Gamba, *Zeolites*, 1987, **7**, 522.
10 P. Demontis, G. B. Suffritti, S. Quartieri, E. S. Fois and A. Gamba, *J. Phys. Chem.*, 1988, **92**, 867.
11 G. Herzberg, *Spectra of Diatomic Molecules*, Van Nostrand Reinhold, New York, 1950.

12 S.-B. Zhu, J. Lee and G. W. Robinson, *Mol. Phys.*, 1988, **65**, 65.
13 S.-B. Zhu and G. W. Robinson, *Comput. Phys. Commun.*, 1989, **52**, 317.
14 S. El Amrani, F. Vigné-Maeder and B. Bigot, *J. Phys. Chem.*, 1992, **96**, 9417.
15 A. V. Kiselev and P. Q. Du, *J. Chem. Soc., Faraday Trans. 2*, 1981, **77**, 1.
16 C. S. Murthy, K. Singer and I. R. McDonald, *Mol. Phys.*, 1981, **44**, 135.
17 M. P. Allen and D. J. Tildesley, *Computer Simulation of Liquids*, Clarendon, Oxford, 1987.
18 S. Bandyopadhyay and S. Yashonath, *J. Phys. Chem.*, 1995, **99**, 4286.
19 M. S. Sun, D. B. Shah, H. H. Xu and O. Talu, *J. Phys. Chem. B*, 1998, **102**, 1466.
20 D. J. Tildesley and P. A. Madden, *Mol. Phys.*, 1981, **42**, 1137.
21 R. Chitra and S. Yashonath, *J. Phys. Chem. B*, 1997, **101**, 5437.
22 R. L. June, A. T. Bell and D. N. Theodorou, *J. Phys. Chem.*, 1992, **96**, 1051.
23 E. Hernández and C. R. A. Catlow, *Proc. R. Soc. London, A*, 1995, **448**, 143.
24 M. Kocirík, J. Kornatowski, V. Masarík, P. Novák, A. Zikánová and J. Maixner, *Micropor. Mesopor. Mater.*, 1998, **23**, 295.
25 J. Kärger, H. Pfeifer, F. Stallmach, N. N. Feoktistova and S. P. Zhdanov, *Zeolites*, 1993, **13**, 50.
26 D. Shen and L. V. C. Rees, *J. Chem. Soc., Faraday Trans.*, 1994, **90**, 3011.
27 J. Caro, M. Bülow, W. Schirmer, J. Kärger, W. Heink and H. Pfeifer, *J. Chem. Soc., Faraday Trans., 1*, 1985, **81**, 2541.
28 J. Kärger and D. M. Ruthven, *Diffusion in Zeolites and Other Microporous Solids*, Wiley, New York, 1992.

Paper a907446e